Available online at www.sciencedirect.com

SciVerse ScienceDirect

Journal of Nutritional Biochemistry 24 (2013) 188–195

Journal of Nutritional Biochemistry

DHA-fluorescent probe is sensitive to membrane order and reveals molecular adaptation of DHA in ordered lipid microdomains☆

Heather Teague[a], Ron Ross[b], Mitchel Harris[a], Drake C. Mitchell[b], Saame Raza Shaikh[a,*]

[a]Department of Biochemistry and Molecular Biology, East Carolina Diabetes and Obesity Institute, East Carolina University, NC 27834, USA
[b]Department of Physics, Portland State University, OR 97201, USA

Received 20 December 2011; received in revised form 11 April 2012; accepted 18 April 2012

Abstract

Docosahexaenoic acid (DHA) disrupts the size and order of plasma membrane lipid microdomains *in vitro* and *in vivo*. However, it is unknown how the highly disordered structure of DHA mechanistically adapts to increase the order of tightly packed lipid microdomains. Therefore, we studied a novel DHA-Bodipy fluorescent probe to address this issue. We first determined if the DHA-Bodipy probe localized to the plasma membrane of primary B and immortal EL4 cells. Image analysis revealed that DHA-Bodipy localized into the plasma membrane of primary B cells more efficiently than EL4 cells. We then determined if the probe detected changes in plasma membrane order. Quantitative analysis of time-lapse movies established that DHA-Bodipy was sensitive to membrane molecular order. This allowed us to investigate how DHA-Bodipy physically adapted to ordered lipid microdomains. To accomplish this, we employed steady-state and time-resolved fluorescence anisotropy measurements in lipid vesicles of varying composition. Similar to cell culture studies, the probe was highly sensitive to membrane order in lipid vesicles. Moreover, these experiments revealed, relative to controls, that upon incorporation into highly ordered microdomains, DHA-Bodipy underwent an increase in its fluorescence lifetime and molecular order. In addition, the probe displayed a significant reduction in its rotational diffusion compared to controls. Altogether, DHA-Bodipy was highly sensitive to membrane order and revealed for the first time that DHA, despite its flexibility, could become ordered with less rotational motion inside ordered lipid microdomains. Mechanistically, this explains how DHA acyl chains can increase order upon formation of lipid microdomains *in vivo*.

Keywords: Lipid microdomains; DHA; Molecular order; Plasma membrane

1. Introduction

The translation of n-3 polyunsaturated fatty acids (PUFAs) into clinical trials for the treatment of chronic inflammation requires a basic understanding of their molecular mechanisms [1]. The mechanisms of n-3 PUFAs are complex and pleiotropic. One mode of action, central to regulating most downstream mechanisms, is the ability of n-3 PUFA acyl chains to disrupt the biophysical properties of the plasma membrane [2]. Many studies show that docosahexaenoic acid (DHA), in particular, can manipulate the formation of membrane signaling microdomains (i.e., signalosomes, caveolae and rafts) [2]. The mechanism by which DHA, either upon transport as a fatty acid through the membrane or upon esterification into phospholipids, disrupts membrane microdomain properties remains incomplete [3,4]. Specifically, it is unknown how DHA, a highly flexible structure, is capable of exerting an ordering effect upon formation of highly packed lipid microdomains [5].

Several methodological issues have prevented a comprehensive understanding of how DHA targets membrane microdomain organization. One major limitation is the lack of appropriate fluorescence tools to study DHA, especially as it relates to determining the physical properties of membranes containing DHA. A few fluorescently labeled fatty acid probes have been used for successfully studying some aspects of n-3 fatty acid biology [6,7]. For instance, such probes have been employed in binding assays to show low K_d values for unsaturated fatty acids binding with PPARα compared to saturated fatty acids [8]. However, the use of PUFAs labeled with fluorescent probes to study membrane microdomain organization has remained elusive.

We have established *in vitro* with EL4 cells and *in vivo* with B cells that DHA disrupts lipid microdomain size and exerts an ordering effect upon cross-linking GM1 molecules relative to no cross-linking [5,9]. Unexpectedly, while studying membrane organization of B cells, we discovered an n-3 PUFA diet lowered the uptake of a Bodipy fluorophore [10]. This finding prompted the current study to determine the potential utility of a Bodipy-labeled fluorophore as a probe for addressing several unresolved mechanistic

☆ This work was supported by a grant from the National Institutes of Health (R15AT006122) to S.R.S. and Oregon Nano and Micro Initiative (ONAMI) to D.C.M. There are no conflicts of interest, and all authors have approved the manuscript.
* Corresponding author. Tel.: +1 252 744 2585; fax: +1 252 744 3383.
E-mail address: shaikhsa@ecu.edu (S.R. Shaikh).

0955-2863/$ - see front matter © 2013 Elsevier Inc. All rights reserved.
http://dx.doi.org/10.1016/j.jnutbio.2012.04.010

questions on how DHA's flexible structure adapts to the formation of ordered lipid microdomains.

The goals of this study were to address the following questions: Does DHA-Bodipy localize to the plasma membrane? Could DHA-Bodipy detect changes in membrane order in cells and in model membranes? If so, could the probe be utilized to provide a potential mechanism by which DHA physically reorients itself within ordered microdomains to increase order? The approach relied on live and fixed cell imaging and time-resolved fluorescence anisotropy methods applied to model membranes (lipid vesicles of controlled composition). The rationale for selecting model membranes was that it is very difficult to study DHA's molecular behavior in ordered and disordered microdomains in cells. The data revealed a mechanistic explanation on how DHA's rotational diffusion and molecular ordering behavior conforms to the ordered lipid microdomain environment.

2. Materials and methods

2.1. Materials

1-Palmitoyl-2-oleoyl-phosphatidylcholine (POPC) and 1-stearoyl-2-docosahexaenoyl-phosphatidylcholine (SDPC) were purchased from Avanti Polar Lipids. Cholesterol (Chol) was purchased from Sigma. 4,4-Difluoro-5,7-dimethyl-4-bora-3a,4a-diaza-sindacene-3-docosahexaenoic acid (DHA-Bodipy), MitoTracker and ER-Tracker were purchased from Invitrogen. DHA-Bodipy was custom synthesized by Invitrogen under stringent conditions to prevent oxidation of the fatty acid. Spectral properties of the probe were determined by adding 1 μl of DHA-Bodipy to 50 μl of phenol-free media in a 96-well flat-bottom plate. The excitation and emission peaks were measured using a SpectraMax Gemini (Molecular Devices) and acquired using Softmax Pro software. The collected data were then imported into GraphPad Prism followed by two-point smoothing analysis.

2.2. Cells

EL4 cells were maintained in RPMI 1640 1× media supplemented with 10% heat-inactivated defined fetal bovine serum (FBS) (Hyclone), 2 mM L-glutamine and 1% penicillin/streptomycin at 37°C in a 5% CO_2 incubator. Primary $B220^+$ B cells were isolated from the spleens of C57BL/6 mice using methods established previously [10].

2.3. Imaging

The concentration of DHA-Bodipy was optimized for each cell type and experiment. Splenic B cells were treated with 1.5 μM of DHA-Bodipy in phenol-free RPMI supplemented with 2 mM L-glutamine at 37°C for 1, 10 and 20 min. B cells were fixed for 1 h with 4% paraformaldehyde, washed three times with 1× phosphate-buffered saline, mounted on slides in Vitrotubes (Fiber Optic Center, Inc.) and imaged using a Zeiss LSM510 confocal microscope [9]. Live cell imaging experiments were also conducted using a Zeiss LSM510 confocal microscope using stage/objective heaters set at 37°C or 23°C. For co-localization studies, 2.0×10^6 EL4 cells at 1.0×10^6 cells/ml were treated with 1.3 μM DHA-Bodipy for 24 h. EL4 cells were counted, washed twice with either Hanks Balanced Salt Solution (HBSS, plus calcium chloride and magnesium chloride) for ER-Tracker staining or RPMI 1640 1× media supplemented with 10% heat-inactivated defined FBS (Hyclone), 2 mM L-glutamine and 1% penicillin/streptomycin (for MitoTracker staining) to remove excess probe. Cells were then resuspended at 1.0×10^6 cells/ml and stained with either 150 nM MitoTracker in RPMI 1640 1× media supplemented with 10% heat-inactivated defined FBS (Hyclone), 2 mM L-glutamine and 1% penicillin/streptomycin, or 2 μM ER-Tracker in HBSS at 37°C for 30 min. Cells were washed twice with phenol-free RPMI with L-glutamine and then placed in a preheated petri dish on the stage heater, followed by image acquisition.

The rate of DHA-Bodipy uptake was measured in EL4 cells adhered to poly-D-lysine-coated Delta T dishes (Bioptechs). Delta T dishes were coated with poly-D-lysine (Sigma) for 15 min, rinsed with water and air-dried overnight. A total of 1.0×10^6 EL4 cells were washed twice with phenol-free RPMI supplemented with 0.5% FBS and 2 mM L-glutamine and resuspended. A total of 1.0×10^6 EL4 cells were added to poly-D-lysine-coated dishes and incubated for 30 min at 37°C to achieve maximum adherence. Imaging was initiated at 1 min following addition of 1.5 μM of DHA-Bodipy to Delta T dishes.

2.4. Image analysis

For the plasma membrane and intracellular intensity analyses, following background subtraction, a region of interest (ROI) was drawn around either the plasma membrane or the intracellular region, and the intensity was measured for each individual cell. For co-localization analysis, each image was background subtracted and then cropped to a 150×150-pixel ROI to analyze each cell individually. Images were then loaded into the National Institutes of Health (NIH) ImageJ JACoP plug-in, the proper threshold was determined, and Manders coefficients (M1 and M2) were calculated based on the thresholded region [9,11]. The rate of DHA-Bodipy uptake was determined by measuring the fluorescence intensity increase over a 25-min time period at 37°C or 23°C. Fluorescence values were normalized relative to maximal fluorescence intensity.

2.5. Preparation of large unilamellar vesicles

Lipid stock solutions with and without added cholesterol were dried from chloroform under a stream of Argon gas, and the resulting phospholipid film was dissolved in cyclohexane. The cyclohexane solution was frozen and then lyophilized for 4 to 5 h. The resulting powder was dispersed in buffer (10 mM PIPES, 60 mM NaCl, 30 mM KCl, 50 mM DTPA, pH 7.3) and put through 8 to 10 freeze–thaw cycles to form multilamellar vesicles. Large unilamellar vesicles were formed by extrusion 10× through a pair of 0.2-μm membranes using a Lipex extruder (Vancouver, BC, Canada). All buffers were heavily flushed with argon immediately prior to use, and all preparative procedures involving unsaturated phospholipids were carried out in an argon-filled glove box. Samples for fluorescence measurements were made immediately prior to use by diluting a concentrated vesicle stock solution to 150 μM phospholipid. Total optical density (vesicle scatter plus absorption) at the wavelength of fluorescence excitation was less than 0.1.

2.6. Time-resolved fluorescence measurements

Fluorescence lifetime and differential polarization measurements were performed with a Chronos multifrequency cross-correlation phase fluorometer (ISS, Urbana, IL, USA). Excitation at 473 nm was provided by a diode laser. Lifetime and differential polarization data were acquired using decay acquisition software from ISS at 10°C, 23°C and 37°C. Both lifetime and differential polarization measurements were acquired at 15 modulation frequencies logarithmically spaced from 5 to 250 MHz. All lifetime measurements were made with the emission polarizer at an angle of 54.7° relative to the vertically polarized excitation beam and with fluorescein in pH 8.0 buffer in the reference cuvette. For each differential polarization measurement, the instrumental polarization factors were measured and found to be between 1 and 1.05, and the appropriate correction factor was applied. Scattered excitation light was removed from the emission beam by a 510-nm high-pass filter in the emission beam. At each frequency, data were accumulated until the standard deviations of the phase and modulation ratio were below 0.2° and 0.004, respectively, and these values were used as the standard deviation for the measured phase and modulation ratio in all analysis. Both total intensity decay and differential polarization measurements were repeated at each temperature, with each membrane composition, a minimum of three times.

2.7. Analysis of time-resolved fluorescence data

Fluorescence lifetimes were analyzed in terms of a sum of two exponential decays of the form: $I(t)=\alpha1\times e^{-t/\tau1}+\alpha2\times e^{-t/\tau2}$, where $\alpha1$ and $\alpha2$ are the fractional contributions to the intensity decay and $\tau1$ and $\tau2$ are time constants. To facilitate comparison of fluorescence lifetimes, the intensity-weighted average fluorescence lifetime, $\langle\tau\rangle$, was determined for each sample.

$$\langle\tau\rangle = \sum_i \frac{\alpha_i\tau_i^2}{\alpha_i\tau_i}$$

Measured polarization-dependent differential phases and modulation ratios for each sample were combined with the measured total intensity decay to yield the anisotropy decay, $r(t)$. Anisotropy decays were analyzed using a sum of two discrete exponential decays of the form:

$$r(t) = (r_o - r_\infty)(\beta_1 exp(-t/\phi_1) + \beta_2 exp(-t/\phi_2)) + r_\infty,$$

where r_o is the initial fluorescence anisotropy at $t=0$, r_∞ is the nondecaying anisotropy remaining at the longest time measured in the experiment, ϕ_i is the ith rotational correlation time and β_i is fractional contribution of the ith component. In order to compare fluorescent probe rotational motion and orientational order, we report the average rotational correlation time $\langle\phi\rangle$ and the order parameter S, respectively [12].

$$\langle\phi\rangle = \sum_i \beta_i\phi_i$$

$$S = \sqrt{\frac{r}{r_o}}$$

2.8. Statistical analyses

The reported data are for three to four independent experiments. Data were analyzed using NIH ImageJ, GraphPad Prism and Excel. All of the data were distributed normally. For analysis of probe organization in model membranes, data were analyzed using a one-way analysis of variance followed by a Bonferroni t test.

3. Results

3.1. Spectral properties of DHA-Bodipy

The structure of DHA-Bodipy is shown in Fig. 1A. The fluorophore was not attached on the terminal methyl end of the fatty acid in order to avoid potential artifacts of the fluorophore on the dynamics of the acyl chain. The excitation maximum for the probe was 501 nm, and the emission was measured at 515 nm (Fig. 1B). The excitation and emission wavelengths were in agreement with the manufacturer's reported values and with reported values for other Bodipy fluorophores [13,14].

3.2. DHA-Bodipy incorporated into the plasma membrane of primary B cells more efficiently than EL4 cells

We first determined if DHA-Bodipy localized into the plasma membrane of primary naive B cells. This was essential to establish in order to use the probe for addressing questions related to how DHA adapts to ordered lipid microdomains. Cells were treated with DHA-Bodipy for 1, 10, and 20 min at 37°C (Fig. 2A). Quantitative analysis of fluorescence intensities revealed that DHA-Bodipy incorporated into the plasma membrane (Fig. 2B). Over time, the fluorescence intensity increased in the plasma membrane and inside the cell (Fig. 2B). However, the ratio of plasma membrane fluorescence intensity to intracellular intensity was relatively constant between 1, 10 and 20 min (Fig. 2C). Therefore, the cells took up more DHA-Bodipy over time but relatively equal amounts into the plasma membrane and inside the cell.

We next determined if EL4 cells also took up DHA-Bodipy into the plasma membrane. The rationale for selecting EL4 cells was that we have previously used this cell type in several studies to compare our results with B cells [5,10]. DHA-Bodipy was rapidly internalized into the cell and showed less staining in the plasma membrane compared to B cells (Supplemental Fig. 1A and Supplemental Movie). We conducted co-localization image analysis to determine where DHA-Bodipy localized to inside the cell after long-term treatment. Co-localization analysis revealed DHA-Bodipy co-localized with the ER (Supplemental Fig. 1B), with ~70% of total DHA-Bodipy co-localizing with the ER according to M2 (Supplemental Fig. 1D), which is the amount of co-localized DHA-Bodipy relative to total DHA-Bodipy present. M1 showed that ~80% of ER-Tracker co-localized with DHA-Bodipy compared to the total amount of ER-Tracker staining (Supplemental Fig. 1D). Co-localization between DHA-Bodipy and the MitoTracker was also observed (Supplemental Fig. 1C), revealing ~40% of DHA-Bodipy (M2) relative to total DHA-Bodipy exhibited colocalization (Supplemental Fig. 1E). M1 showed that ~70% of MitoTracker co-localized with DHA-Bodipy compared to total MitoTracker present (Supplemental Fig. 1E).

3.3. DHA-Bodipy was sensitive to membrane order in cells and model membranes

The subsequent set of experiments addressed if DHA-Bodipy was sensitive to membrane order. Therefore, the rate of DHA-Bodipy uptake was measured in real time at 37°C and 23°C using EL4 cells. EL4 cells were used since they showed rapid uptake of DHA-Bodipy into the cell. The two temperatures were selected since the plasma membrane is highly fluid at 37°C, whereas at 23°C, the membrane is more ordered [2]. Fig. 3A shows the uptake of DHA-Bodipy over time into the cell. Kinetic fitting of fluorescence intensity values revealed that the rate of DHA-Bodipy uptake was the same at 37°C and 23°C (data not shown). However, the magnitude of probe uptake was much lower at 23°C relative to 37°C, demonstrating that the probe was sensitive to plasma membrane molecular order (Fig. 3B).

The DHA-Bodipy was then used to determine if the probe was sensitive to order in model membranes (Fig. 3C). The rationale for

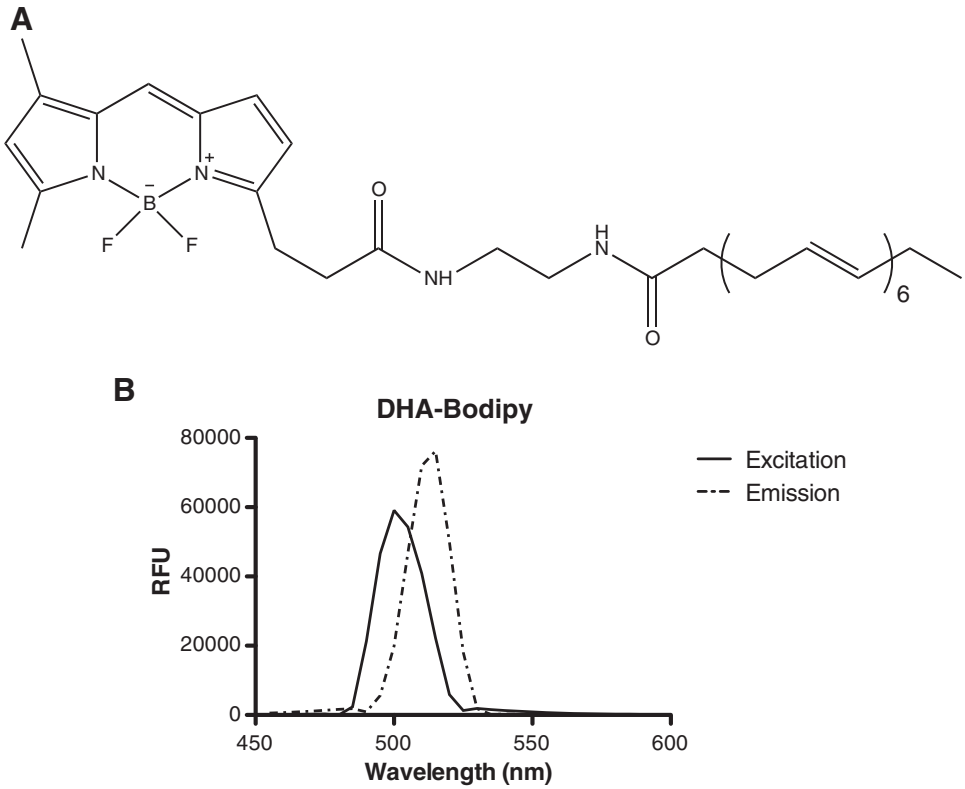

Fig. 1. Structure and spectral properties of DHA-Bodipy. (A) Structure of DHA-Bodipy used in this study. (B) Spectral properties of the probe in terms of relative fluorescence units (RFU). The probe was custom synthesized with the fluorophore away from the terminal methyl end in order to avoid any potential effects of the bulky group on the dynamics of the acyl chain, which was the focus of this study. Data in B are representative of three individual measurements.

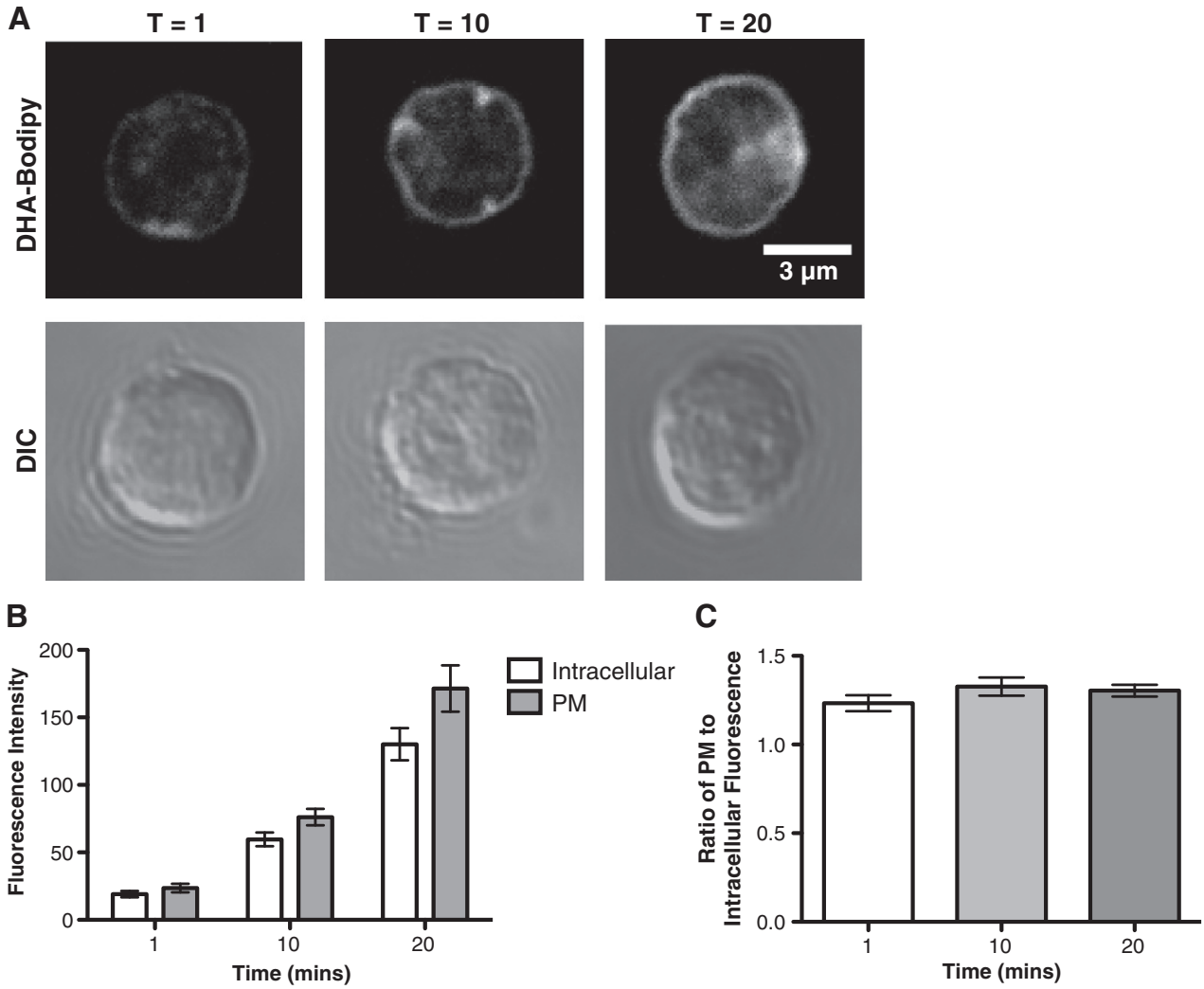

Fig. 2. DHA-Bodipy incorporates into the plasma membrane of primary B cells. (A) Sample fluorescent and DIC images of DHA-Bodipy localizing to the plasma membrane (PM) of primary B cells as a function of time at 37°C. (B) Quantification of PM and intracellular DHA-Bodipy total fluorescence intensity as a function of time. (C) Ratio of PM to intracellular DHA-Bodipy fluorescence as a function of time. B cells were stained at 37°C. Data are average±S.E. from three independent experiments.

using model membranes was that we wanted to determine if the probe could provide novel mechanistic information about DHA in highly disordered and ordered microdomains, which respectively model nonraft and raft-like membranes. Therefore, we used three different types of lipid vesicles that represented highly ordered (POPC/Chol), disordered (POPC) and highly disordered (SDPC) microdomains [15,16]. To verify that the probe was sensitive to membrane phase behavior, we measured the steady-state anisotropy in the fluid (37°C) and ordered (23°C) environments, similar to the cell culture studies (Fig. 3A,B). Analysis of steady-state anisotropies showed that in POPC and POPC/Chol vesicles anisotropy values were lower at 37°C than 23°C, consistent with more disorder at a higher temperature (Fig. 3C). SDPC vesicles showed a similar trend as POPC and POPC/Chol, but the differences between temperatures were smaller. This was probably due to high molecular disorder in SDPC.

3.4. DHA-Bodipy revealed novel molecular organization in ordered lipid microdomains

Finally, we used DHA-Bodipy to measure its molecular order and rotational motion in ordered and disordered domains at 37°C, 23°C and 10°C. This question was highly relevant since the mechanism by which the flexible structure of DHA increases the order of lipid microdomains has not been investigated and has remained controversial [3,17]. We used SDPC as the control for these studies since this represented the disordered microdomain that contained a phosphatidylcholine with DHA.

Fluorescence lifetimes were lowered at all temperatures in POPC vesicles but were higher in POPC/Chol relative to SDPC (Fig. 4). This suggested that, in the most ordered membrane, the DHA-Bodipy had the least interaction with the surrounding water environment. This would be consistent with the DHA fatty acid being lower in the membrane.

We also measured fluorescence order parameters and rotational correlation times (Fig. 5). As the temperature was lowered from 37°C to 10°C, both the order parameters and rotational correlation times increased (Fig. 5A–C). The changes in temperature provided an internal control by demonstrating that a decrease in temperature increased the average orientational order and decreased its rate of rotational motion in all three lipid compositions (SDPC, POPC and POPC/Chol). For most of the temperatures, order parameters and rotational correlation times were increased in POPC vesicles relative to SDPC (Fig. 5A–C). For all temperatures, order parameters and rotational correlation times were generally

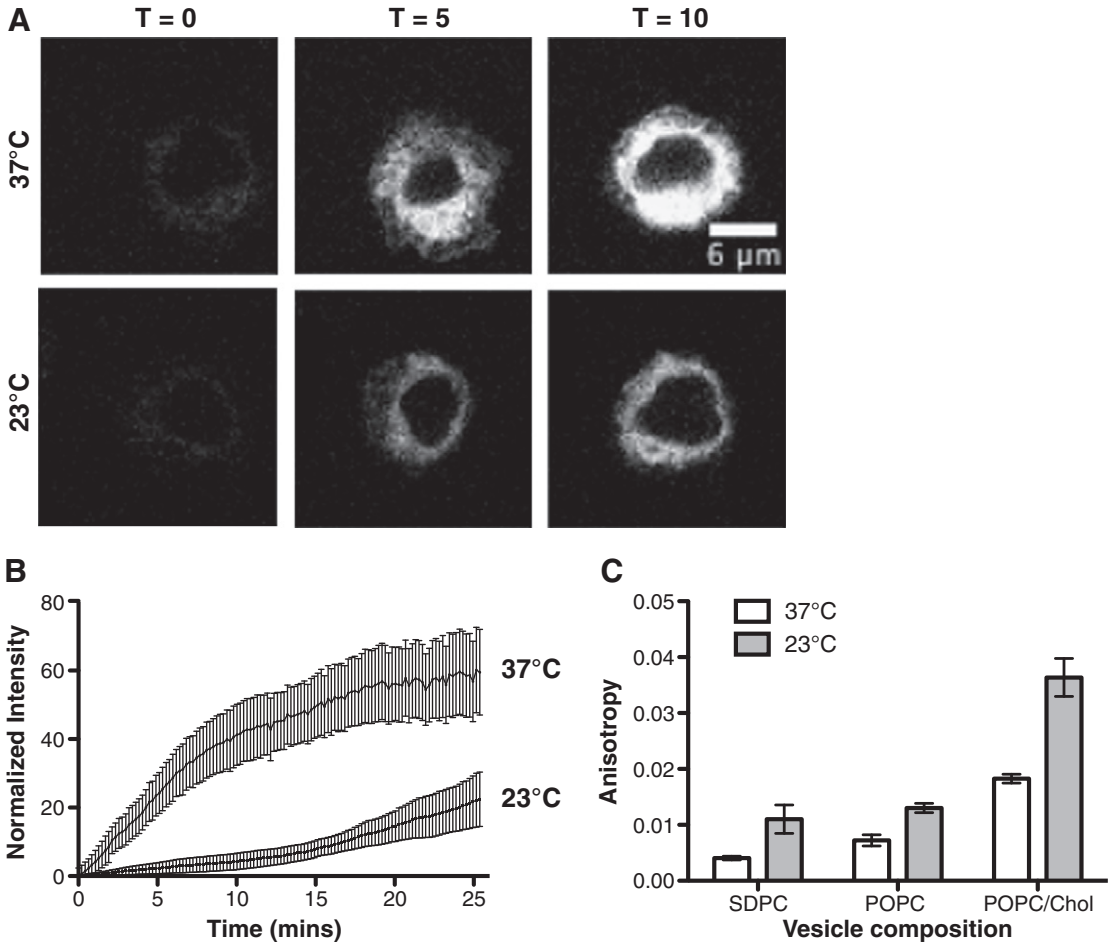

Fig. 3. DHA-Bodipy is sensitive to membrane order in cells and lipid vesicles. (A) Sample time-lapse images showing uptake of DHA-Bodipy into EL4 cells at 37°C and 23°C upon addition of the probe. (B) Quantification of fluorescent probe uptake as a function of time at 37°C and 23°C. Fluorescence values were normalized to maximal fluorescence. (C) Steady-state anisotropy values for SDPC, POPC and POPC/Chol vesicles at 37°C and 23°C. Data are average±S.E. from three to four independent experiments.

increased for POPC/Chol relative to SDPC (Fig. 5A–C). The two most robust differences were the high values of the order parameter in POPC/Chol and the fast rotational motion (low rotational correlation time) found in SDPC. This demonstrated that DHA-Bodipy displayed increased order and slower rotational motion in more ordered POPC and highly ordered POPC/Chol membranes relative to SDPC.

4. Discussion

In this study, we relied on a new DHA-labeled fluorophore to measure uptake into the plasma membrane, sensitivity to membrane order in cells and model membranes, and dynamic organization in model lipid microdomains. The data revealed that DHA lowered its rotational diffusion and increased its molecular ordering in an ordered lipid microdomain environment. The results provide novel mechanistic insight on how DHA acyl chains, despite their high degree of conformational flexibility, could increase their molecular order upon the formation of lipid microdomains *in vivo*.

4.1. DHA incorporation into naive B and EL4 cells

The first set of studies established that DHA-Bodipy, upon short-term treatment, incorporated into the plasma membrane of primary B cells. We ensured that the probe was localizing into the plasma membrane and remained in the plasma membrane in primary B cells. We also observed similar effects in experiments with splenocytes (data not shown). Given the structure of the probe, we did not anticipate DHA-Bodipy to become esterified into phospholipids since the fluorophore was located in the head-group region. We intentionally designed the fluorophore to be localized to the head-group region rather than the terminal methyl end since we aimed to investigate the molecular motions of the acyl chains. One alternative possibility was to place the Bodipy on a phosphatidylethanolamine (PE) head-group; however, this probe could have been difficult to study since DHA-containing PEs can form inverted hexagonal phase [15]. Overall, our results were consistent with our previous study in which we showed another Bodipy probe could localize to the plasma membrane [18].

In EL4 cells, the DHA-Bodipy probe did not show efficient localization into the plasma membrane upon short-term treatment. This showed that the probe's behavior was cell type dependent. This is consistent with studies, including our own, that have demonstrated differences between primary and immortal cell types [10]. The finding that DHA-Bodipy, upon long-term treatment, localized into endomembranes was consistent with previous measurements with palmitic-acid-labeled Bodipy (PA-Bodipy). For instance, Thumser and Storch showed that PA-Bodipy did not esterify into membrane phospholipids in Caco-2 cells, but the probe did report identically to an endogenous palmitic acid [13]. Furthermore, they also showed the probe co-localized with endomembranes and the fatty acid binding protein [13]. To ensure that our methods did not confound our results, we also conducted select studies with PA-

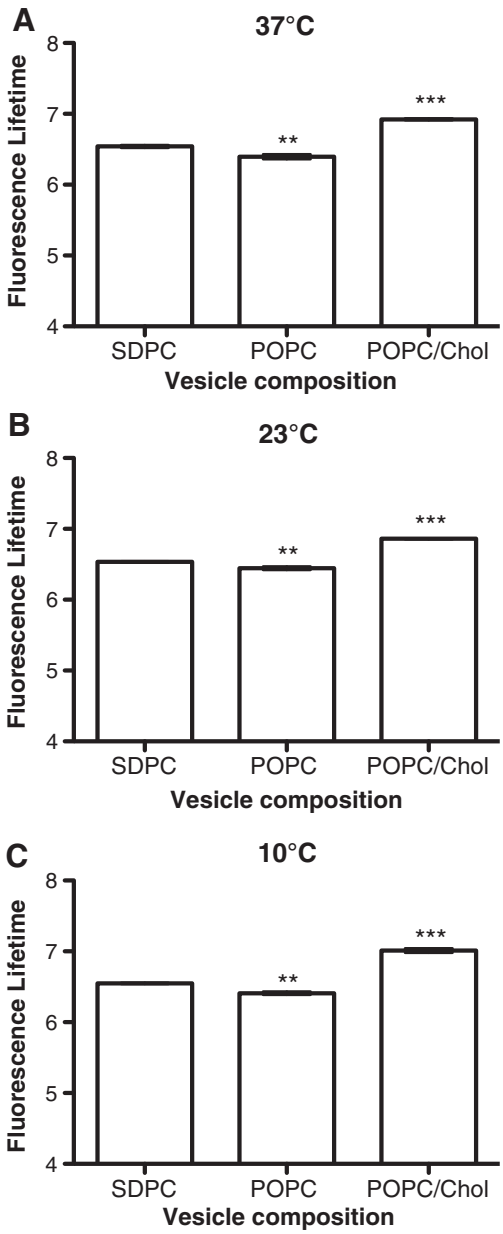

Fig. 4. DHA-Bodipy has higher fluorescence lifetimes in ordered domains compared to disordered domains. Fluorescence lifetime of the DHA-Bodipy probe was measured using time-resolved fluorescence anisotropy in lipid vesicles of defined composition at (A) 37°C, (B) 23°C and (C) 10°C. POPC/Chol, POPC and SDPC, respectively, represent highly ordered, disordered and highly disordered membrane domains. Data are average±S.E. from three independent experiments. Asterisks indicate significance from SDPC: $^{**}P<.01$; $^{***}P<.001$.

Bodipy and indeed found very similar results to those reported by Thumser and Storch (data not shown). It is important to note that our study was the first, to the best of our knowledge, to study a DHA-labeled Bodipy fluorophore.

The long-term treatment studies with DHA-Bodipy highlighted a potential new area of investigation, that is, the ability of DHA to target intracellular membrane organization. The data raised the possibility that some fraction of DHA localizes in some cell types into the ER and mitochondrial membranes, where it is plausible that the fatty acid exerts it effects on membrane organization and function [19]. Some studies do show that DHA can manipulate membrane viscosity of the mitochondrial membrane but have not provided mechanistic details [20]. It is conceivable that DHA could be targeting mitochondrial membrane protein clustering and thereby bioenergetics, which has consequences for ATP production via the electron transport chain [19]. We aim to pursue how DHA targets endomembrane organization in the future.

4.2. DHA's flexible structure adapts to the ordered nature of lipid microdomains

The next set of experiments specifically addressed if DHA-Bodipy was sensitive to membrane order in cells and model membranes. These experiments were essential in order to determine if DHA-Bodipy could be used to study its dynamics within ordered lipid microdomains. Indeed, DHA-Bodipy was sensitive to membrane order as uptake of the probe into EL4 cells was lowered in an ordered environment, created by lowering the temperature to 23°C. Several models of fatty acid uptake, which are not entirely in agreement, have been proposed for long-chain fatty acids [21,22]. These models include free diffusion of fatty acids or uptake mediated by specific proteins such as fatty acid binding proteins. In the future, we aim to use this probe to study the transport of DHA into varying cell types.

The data on membrane order provided novel insight about our previous studies. We previously reported that a high dose of n-3 PUFAs administered to mice prevented the short-term uptake of PA-Bodipy into B cells, relative to a control diet [10]. Our data here implied that a reduction in uptake could take place in response to an increase in membrane molecular order. Thus, we speculate that n-3 PUFAs *in vivo*, upon formation of lipid microdomains, may be increasing their molecular order, perhaps by some interactions with cholesterol [5,23–25]. This would be highly consistent with data showing that n-3 PUFAs increased the molecular order of rafts on the $CD4^+$ T-cell side of the immunological synapse [26] or increased membrane order, as we demonstrated, upon cross-linking GM1 microdomains of B cells [5].

Lipid vesicles of defined composition were employed to further study if the probe was sensitive to highly ordered (POPC/Chol), disordered (POPC) and highly disordered (SDPC) domains [15,16,27,28]. These studies demonstrated that the probe was indeed sensitive to molecular order in model membranes, which was evident from changes in temperature and changes in lipid composition.

The time-resolved anisotropy results revealed new mechanistic insight into how DHA behaved when interacting with ordered microdomains. Specifically, we discovered that DHA-Bodipy became ordered in POPC and POPC/Chol vesicles relative to SDPC. This provided evidence that DHA acyl chains, albeit highly disordered, can adapt and interact with ordered lipid microdomains and, in fact, can undergo an increase in molecular order inside an ordered domain [3]. While some biochemical and biophysical studies show that DHA prefers to avoid interactions with cholesterol [4], our data suggest that when forced into a raft-like ordered environment, the acyl chain surprisingly is capable of adapting to this environment, which will impact the clustering and activity of surrounding proteins [3]. Our data are also consistent with a recent study showing that cholesterol could increase the order of DHA esterified to phosphatidylcholines [25]. This helps explain how n-3 PUFAs *in vivo* appear to make rafts larger and more ordered [10,26].

There are many important questions that remain unanswered about the mechanistic relationship between DHA and ordered domains that could be addressed in the future with this DHA-labeled fluorophore. For simplicity, we present two examples. One, it is conceivable that DHA's initial uptake through the membrane as a fatty acid could selectively manipulate the organization of membrane microdomains, clustering of proteins and/or lateral diffusion of membrane molecules. Second, the existing environment itself could

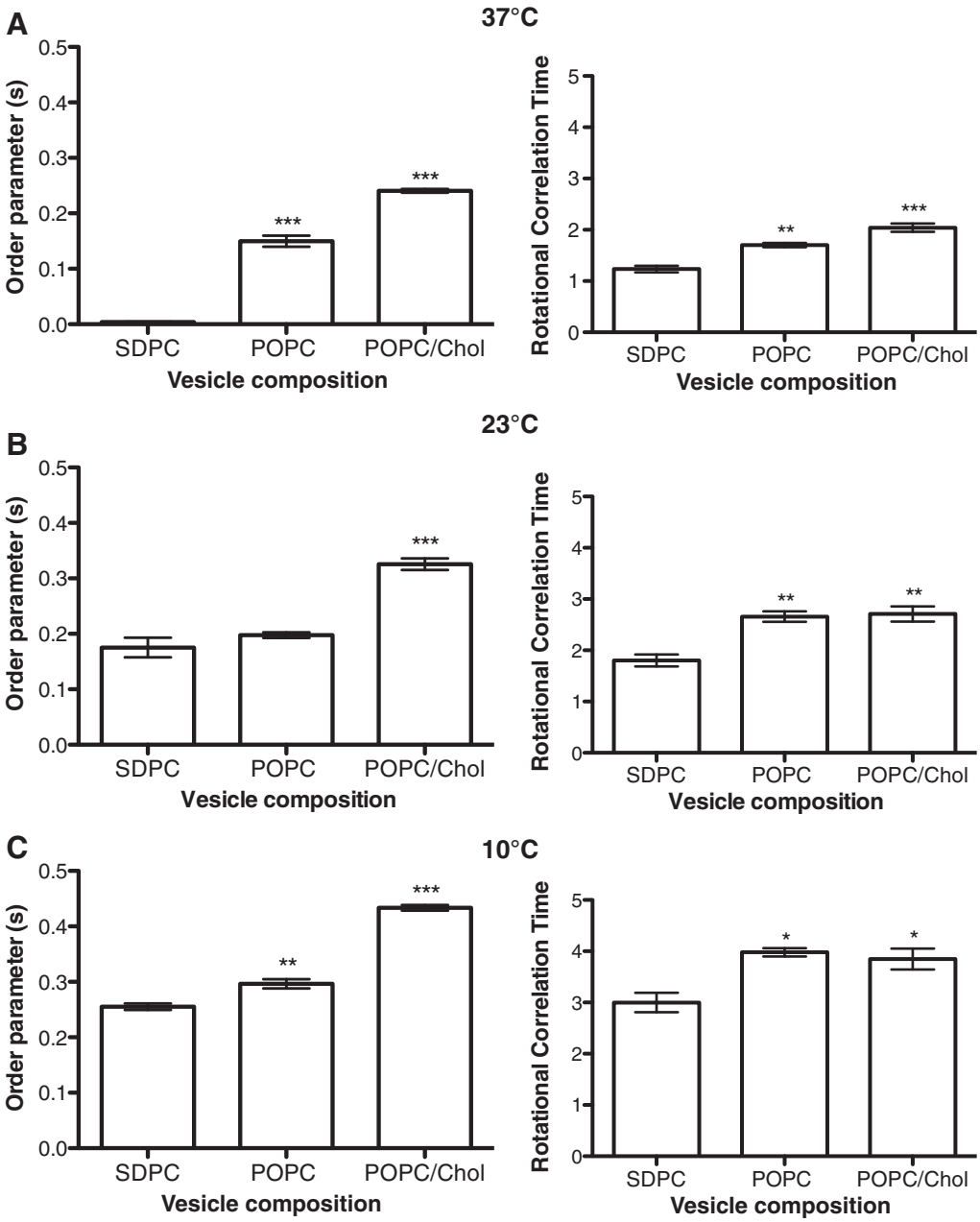

Fig. 5. DHA-Bodipy displays increased order and decreased rotational diffusion in ordered lipid microdomains. Order parameters and rotational correlation times for the DHA-Bodipy probe were determined using time-resolved fluorescence anisotropy in lipid vesicles of defined composition at (A) 37°C, (B) 23°C and (C) 10°C. POPC/Chol, POPC and SDPC, respectively, represent highly ordered, disordered and highly disordered membrane domains. Data are average±S.E. from three independent experiments. Asterisks indicate significance from SDPC: *P<.05; **P<.01; ***P<.001.

influence the uptake of DHA into the membrane. For example, macrophages that are deficient in the cholesterol transporter ABCA1 have larger lipid rafts due to increased accumulation of cholesterol [29,30]. This increase in molecular order of the plasma membrane would then have an impact on the uptake of fatty acids into the cell including DHA. Thus, the order of the membrane itself would influence the uptake kinetics of DHA and could limit bioavailability of the fatty acid for the cell.

4.3. Summary

We have demonstrated for the first time that a new DHA-Bodipy was sensitive to membrane order in both cells and lipid vesicles of defined composition. We then discovered that the highly flexible structure of DHA adapted within ordered lipid microdomains by increasing its molecular order and lowering its rotational diffusion. This now explains mechanistically how DHA can increase lipid microdomain molecular order *in vivo*.

Supplementary data to this article can be found online at http://dx.doi.org/10.1016/j.jnutbio.2012.04.010.

Acknowledgments

We thank Dr. Bill Stillwell for his useful suggestions and interpretation of the data. We also thank Benjamin Drew Rockett for his assistance in developing the microscopy studies.

References

[1] Chapkin RS, McMurray DN, Davidson LA, Patil BS, Fan YY, Lupton JR. Bioactive dietary long-chain fatty acids: emerging mechanisms of action. Br J Nutr 2008;100:1152–7.

[2] Stillwell W, Wassall SR. Docosahexaenoic acid: membrane properties of a unique fatty acid. Chem Phys Lipids 2003;126:1–27.

[3] Shaikh SR, Jolly CA, Chapkin RS. n-3 Polyunsaturated fatty acids exert immunomodulatory effects on lymphocytes by targeting plasma membrane molecular organization. Mol Aspects Med 2011;33:46–54.

[4] Shaikh SR. Biophysical and biochemical mechanisms by which dietary N-3 polyunsaturated fatty acids from fish oil disrupt membrane lipid rafts. J Nutr Biochem 2012;23:101–5.

[5] Rockett BD, Teague H, Harris M, Melton M, Williams J, Wassall SR, et al. Fish oil increases raft size and membrane order of B cells accompanied by differential effects on function. J Lipid Res 2012;53:674–85.

[6] Stillwell W, Jenski LJ, Zerouga M, Dumaual AC. Detection of lipid domains in docasahexaenoic acid-rich bilayers by acyl chain-specific FRET probes. Chem Phys Lipids 2000;104:113–32.

[7] McIntosh AL, Huang H, Atshaves BP, Wellberg E, Kuklev DV, Smith WL, et al. Fluorescent n-3 and n-6 very long chain polyunsaturated fatty acids: three-photon imaging in living cells expressing liver fatty acid-binding protein. J Biol Chem 2010;285:18693–708.

[8] Lin Q, Ruuska SE, Shaw NS, Dong D, Noy N. Ligand selectivity of the peroxisome proliferator-activated receptor alpha. Biochemistry 1999;38:185–90.

[9] Shaikh SR, Rockett BD, Salameh M, Carraway K. Docosahexaenoic acid modifies the clustering and size of lipid rafts and the lateral organization and surface expression of MHC class I of EL4 cells. J Nutr 2009;139:1632–9.

[10] Rockett BD, Franklin A, Harris M, Teague H, Rockett A, Shaikh SR. Membrane raft organization is more sensitive to disruption by (n-3) PUFA than nonraft organization in EL4 and B cells. J Nutr 2011;141:1041–8.

[11] Bolte S, Cordelieres FP. A guided tour into subcellular colocalization analysis in light microscopy. J Microscopy 2006;224:213–32.

[12] Heyn MP, Cherry RJ, Dencher NA. Lipid–protein interactions in bacteriorhodopsin–dimyristoylphosphatidylcholine vesicles. Biochemistry 1981;20:840–9.

[13] Thumser AE, Storch J. Characterization of a BODIPY-labeled fluorescent fatty acid analogue. Binding to fatty acid-binding proteins, intracellular localization, and metabolism. Mol Cell Biochem 2007;299:67–73.

[14] Karsenty J, Helal O, de la Porte PL, Beauclair-Deprez P, Martin-Elyazidi C, Planells R, et al. I-FABP expression alters the intracellular distribution of the BODIPY C16 fatty acid analog. Mol Cell Biochem 2009;326:97–104.

[15] Shaikh SR, Brzustowicz MR, Stillwell W, Wassall SR. Formation of inverted hexagonal phase in SDPE as observed by solid-state (31)P NMR. Biochem Biophys Res Comm 2001;286:758–63.

[16] Reyes Mateo C, Ulises Acuna A, Brochon JC. Liquid-crystalline phases of cholesterol/lipid bilayers as revealed by the fluorescence of trans-parinaric acid. Biophys J 1995;68:978–87.

[17] Kim W, Khan NA, McMurray DN, Prior IA, Wang N, Chapkin RS. Regulatory activity of polyunsaturated fatty acids in T-cell signaling. Prog Lipid Res 2010;49:250–61.

[18] Shaikh SR, Mitchell D, Carroll E, Li M, Schneck J, Edidin M. Differential effects of a saturated and a monounsaturated fatty acid on MHC class I antigen presentation. Scand J Immunol 2008;68:30–42.

[19] Shaikh SR, Brown DA. Models of plasma membrane organization can be applied to mitochondrial membranes to target human health and disease with polyunsaturated fatty acids. Prostaglandins Leukot Essent Fatty Acids 2012 In Press.

[20] Stillwell W, Jenski LJ, Crump FT, Ehringer W. Effect of docosahexaenoic acid on mouse mitochondrial membrane properties. Lipids 1997;32:497–506.

[21] Hamilton JA. Transport of fatty acids across membranes by the diffusion mechanism. Prostaglandins Leukot Essent Fatty Acids 1999;60:291–7.

[22] Hamilton JA. New insights into the roles of proteins and lipids in membrane transport of fatty acids. Prostaglandins Leukot Essent Fatty Acids 2007;77:355–61.

[23] Chapkin RS, Wang N, Fan YY, Lupton JR, Prior IA. Docosahexaenoic acid alters the size and distribution of cell surface microdomains. Biochem Biophys Acta 2008;1778:466–71.

[24] Schley PD, Brindley DN, Field CJ. (n-3) PUFA alter raft lipid composition and decrease epidermal growth factor receptor levels in lipid rafts of human breast cancer cells. J Nutr 2007;137:548–53.

[25] Mihailescu M, Soubias O, Worcester D, White SH, Gawrisch K. Structure and dynamics of cholesterol-containing polyunsaturated lipid membranes studied by neutron diffraction and NMR. J Mem Biol 2011;239:63–71.

[26] Kim W, Fan YY, Barhoumi R, Smith R, McMurray DN, Chapkin RS. n-3 polyunsaturated fatty acids suppress the localization and activation of signaling proteins at the immunological synapse in murine CD4 + T cells by affecting lipid raft formation. J Immunol 2008;181:6236–43.

[27] Pare C, Lafleur M. Polymorphism of POPE/cholesterol system: a 2H nuclear magnetic resonance and infrared spectroscopic investigation. Biophys J 1998;74:899–909.

[28] de Almeida RF, Loura LM, Fedorov A, Prieto M. Lipid rafts have different sizes depending on membrane composition: a time-resolved fluorescence resonance energy transfer study. J Mol Biol 2005;346:1109–20.

[29] Koseki M, Hirano K, Masuda D, Ikegami C, Tanaka M, Ota A, et al. Increased lipid rafts and accelerated lipopolysaccharide-induced tumor necrosis factor-alpha secretion in Abca1-deficient macrophages. J Lipid Res 2007;48:299–306.

[30] Fessler MB, Parks JS. Intracellular lipid flux and membrane microdomains as organizing principles in inflammatory cell signaling. J Immunol 2011;87:1529–35.